Measurements of Intra-Aortic Balloon Wall Movement During Inflation and Deflation: Effects of Angulation

*Gianpaolo Bruti, *Christina Kolyva, †John R. Pepper, and *Ashraf W. Khir

*Brunel Institute for Bioengineering, Brunel University, Uxbridge; and †NIHR Biological Research Unit, Royal Brompton Hospital, London, UK

Abstract: The intra-aortic balloon pump (IABP) is a ventricular assist device that is used with a broad range of pre-, intra-, and postoperative patients undergoing cardiac surgery. Although the clinical efficacy of the IABP is well documented, the question of reduced efficacy when patients are nursed in the semi-recumbent position remains outstanding. The aim of the present work is therefore to investigate the underlying mechanics responsible for the loss of IABP performance when operated at an angle to the horizontal. Simultaneous recordings of balloon wall movement, providing an estimate of its diameter (D), and fluid pressure were taken at three sites along the intra-aortic balloon (IAB) at 0 and 45°. Flow rate, used for the calculation of displaced volume, was also recorded distal to the tip of the balloon. An in vitro experimental setup was used, featuring physiological impedances on either side of the IAB ends. IAB inflation at an angle of 45° showed that D increases at the tip of the IAB first, presenting a resistance to the flow displaced away from the tip of the balloon. The duration of inflation decreased by 15.5%, the inflation pressure pulse decreased by 9.6%, and volume decreased by 2.5%. Similarly, changing the position of the balloon from 0 to 45°, the balloon deflation became slower by 35%, deflation pressure pulse decreased by 14.7%, and volume suctioned was decreased by 15.2%. IAB wall movement showed that operating at 45° results in slower deflation compared with 0°. Slow wall movement, and changes in inflation and deflation onsets, result in a decreased volume displacement and pressure pulse generation. Operating the balloon at an angle to the horizontal, which is the preferred nursing position in intensive care units, results in reduced IAB inflation and deflation performance, possibly compromising its clinical benefits. **Key Words:** Intra-aortic balloon pump—Pressure—Flow—Operating angle—Balloon diameter—Counterpulsation—Visualization—Inflation—Deflation.

Although the intra-aortic balloon pump (IABP) has been widely used in clinical practice for more than 40 years, the mechanics of balloon inflation and deflation are still not well understood. Of particular relevance is the issue of the IABP's decreased performance when patients are nursed in the semi-recumbent position (1,2), which is the preferred position to avoid respiratory complications (3,4) and to enhance atrial emptying. Specifically, Lorente

et al. (4) suggested that the position of the patient should never be less than 10°. Even though the position at which the patient is kept can change based on their pathology and respective hospital, a semi-recumbent position is indicated for all patients undergoing IABP therapy.

Previous studies aimed at investigating balloon mechanics at the horizontal and angled positions through analyzing qualitatively its wall movement during counterpulsation (5,6). Khir et al. (6) determined that the inflation and deflation patterns are angle dependent. At an angle to the horizontal, the balloon begins to inflate at the tip moving down toward the base, and this sequence is reversed for deflation, due to the hydrostatic pressure difference between the two ends of the balloon. The authors reported that this can lead to a reduction in the performance of the IABP both in terms of coronary flow

and end-diastolic pressure. Bleifeld et al. (5) used a cine-angiographic technique in hydraulic models, at horizontal and vertical positions, to better understand the inflation and deflation behavior of a cylindrical balloon. The authors explained that the trapping phenomenon, in which the tip and the base of the balloon inflate before the rest of the balloon at a horizontal position, disappears when the IABP operates at an angle to the horizontal, due to the pressure difference between the two ends of the intra-aortic balloon (IAB).

Earlier works from our group (6–9) verified that the fluid volumes displaced toward the tip and base of the IAB change with angle; during inflation, an increase in angle resulted in a decrease in volume displaced above the tip of the IAB (6–9) (upstream) and an increase in volume displaced below the base of the IAB where the catheter is attached (downstream). Using high-speed filming, Biglino et al. demonstrated that increasing angle induces an increase in both duration of inflation and deflation (7).

All of the above visualization studies have considered the changes in the balloon wall qualitatively, and not in relation to the pressure and flow on either side of the balloon. Therefore, our understanding of the reasons for the reduced efficiency of inflation and deflation when the balloon is operated at an angled position remains limited.

The aim of this work is then to provide further understanding of IAB wall movement changes and its effects on hemodynamic parameters during inflation and deflation at horizontal and angled positions. To that aim, earlier studies of pressure and flow provided the outcome of operating the balloon at an angle. However, in the current study we seek to provide a detailed examination of the physical phenomena through the measurement of balloon diameter throughout the counter-pulsation cycle at three locations along the balloon. Wall movement measurements will also be supported by fluid pressure measurements at the same locations and flow upstream, with the objective of understating the link between wall movement, its timing in different parts of the balloon, and the associated pressure and flow generated by IAB inflation and deflation.

MATERIALS AND METHODS

Experimental setup

The experimental setup is shown in Fig. 1. A straight silicone rubber tube of 2.3 cm internal diameter, 40 cm in length, and 0.25 cm wall thickness was selected to replicate the aorta (AO). The wall thickness and diameter of the tube were constant along its length to avoid complications with the visualization technique. AO compliance was measured by inserting a volume of 20 mL of water into the already filled up and sealed AO, in four steps of 5 mL, and measuring the corresponding pressure change. The AO compliance was found to be 0.084 mL/mm Hg, comparable
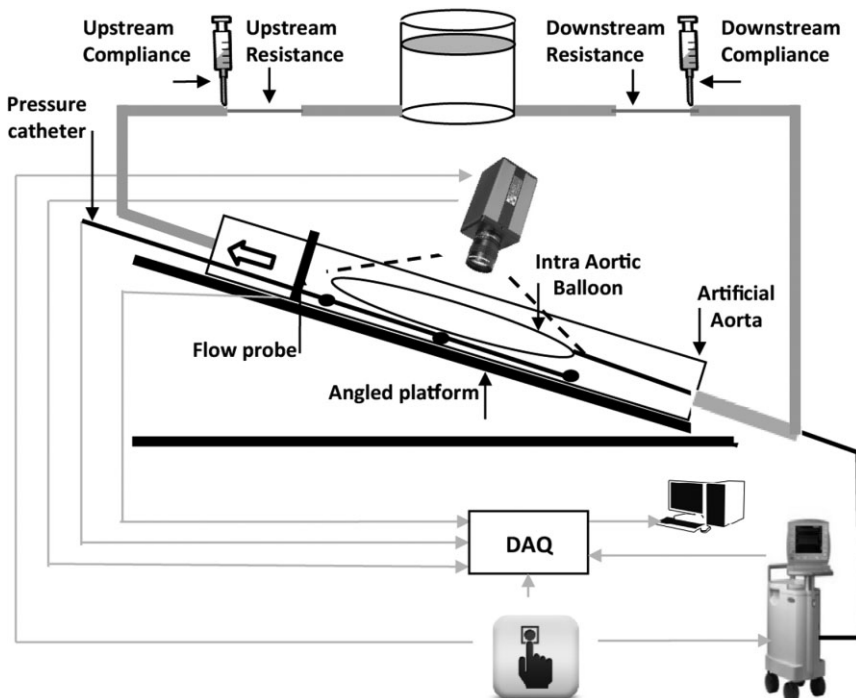

FIG. 1. Schematic of the experimental setup. The reservoir was connected to the artificial aorta (AO) via two polyurethane tubes; two capillary tubes and two air-filled syringes constitute the up- and downstream physiological impedance in terms of resistances and compliances (see Khir et al. [6]). The balloon is placed in the middle of the artificial AO. A pressure catheter is placed along the balloon to measure pressure at the IAB tip, center, and base. The thick arrow indicates the direction upstream of the balloon where a flow probe is snug-fitted to the artificial AO for measuring the volume displaced and suctioned due to inflation and deflation. When the button is pressed, it triggers the IABP, high-speed camera, and data acquisition for simultaneous measurements of the pressure, flow, and balloon filming. The dashed lines indicate the field of view of the camera. The lateral distance between the water level in the reservoir and the center line of the IAB was kept at 1.2 m for both the horizontal angled (0°, 45°) positions by raising the reservoir appropriately to maintain the same static mean pressure at the center of the balloon (90 mm Hg).

with the physiological value of 0.11 mL/mm Hg measured in the thoracic AO, reported by Westerhof et al. (10). The AO and the mock circulation were filled with water, and a Linear 40 cc IAB (Datascope, Fairfield, NJ, USA) with maximum diameter of 1.6 cm and length of 27 cm was placed inside. The AO was placed on a platform, whose angle to the horizontal could be adjusted to resemble different patient postures, and connected to a reservoir. The tubes connecting the AO to the reservoir represented the physiological resistances up- and downstream of the IABP, of 84 and 26 mm Hg × min/L, respectively, reported by Khir (11) who also reported compliances of 8×10^{-3} mL/mm Hg above and 21×10^{-3} mL/mm Hg below the balloon. The resistances and compliances were implemented by attaching capillary tubes and placing air-filled syringes in parallel, up-, and downstream of the IAB. Correspondence between syringe volume and value of compliance was reported by Kolyva et al. (12) during the development of an experimental mock circulation system. The reservoir provided the initial static pressure (P_s) of 90 mm Hg, replicating aortic pressure at the time of the dicrotic notch (generally used as landmark for the onset of balloon inflation). P_s was calculated as $P_s = \rho gh$, where ρ is water density (1000 kg/m^3), g is gravitational acceleration (9.81 m/s^2), and h (1.20 m) is the lateral distance between the water level in the reservoir and the centerline of the balloon (7). For the horizontal and angle 45° positions, h was kept constant by raising the reservoir accordingly to maintain the same static mean pressure at the center of the balloon.

The balloon was connected to an IABP (Datascope CS300), which was triggered through a wave generator replicating a heart rate (HR) of 65 bpm to resemble physiological operating conditions. A high-speed camera (X-PRI, AOS Technologies AG, Baden Daettwil, Switzerland) used for the recording of the balloon wall movement of the longitudinal section of the IAB, at a rate of 500 Hz, was also activated by the pulse generator; in this way, the starting of the IABP trigger and the filming of the balloon were synchronized. Specialized software (AOS Imaging Studio V 2.5.6.1) was used to control the camera and adjust the gray scale and luminosity.

Measurements

A catheter (6 Fr, Gaeltec, Scotland, UK) with three pressure transducers was inserted in the AO and positioned along the balloon in order to measure the pressure at three sites: tip, base, and midpoint. Flow rate upstream of the tip of the balloon was measured through a 28 mm flow probe (28A, Transonic, Ithaca, NY, USA), snug-fitted to the AO at 5 cm away from the tip of the balloon. Uncalibrated helium pressure and pulse generator signal were recorded to indicate landmarks of inflation and deflation, and enable synchronization of all recorded signals, respectively. The pressure and flow signals were acquired at a sampling frequency of 2000 Hz. Five experiments were conducted at the horizontal position and five at an angle of 45°, in each of which the data of 10 consecutive beats were recorded during 1:1 assistance frequency using an analogue-digital converter and Labview software (National Instruments, Austin, TX, USA).

Data analysis

Filter

A Savitzky–Golay low-pass filter (window size = 51, and polynomial order = 2) was used for removing the noise from the pressure and diameter waveforms. No filter was applied on the flow waveform, because the volume calculations from the flow waveform are not affected by white noise.

Pressure and flow data

The inflation and deflation phases for volume calculation were identified on the flow waveform shown in Fig. 2, as the period between point A and point B, and point B and point C, respectively. The volumes displaced (VU) and suctioned from upstream (VS), during inflation and deflation, were calculated by integrating the area below and above, respectively, the flow waveform measured upstream, with respect to time. VU and VS were subsequently normalized as a ratio of the balloon nominal volume (Vn = 40 mL), obtaining the normalized volume displaced (VUTVi) and suctioned (VUTVd) from upstream during inflation and deflation, respectively. We also determined the pressure pulse due to inflation (PPi) and deflation (PPd) at the three measurement sites along the balloon. PPi is calculated as the difference between the pressure value at the onset of inflation and maximum pressure, while PPd is calculated as the difference between the pressure value at the onset of deflation and the minimum pressure value.

The pressure difference between tip and base, which drives the flow along the balloon during inflation and deflation, has also been calculated.

Images

Diameter at three locations along the balloon, tip, base, and midpoint, was determined by offline tracking in the videos recorded by the high-speed camera,
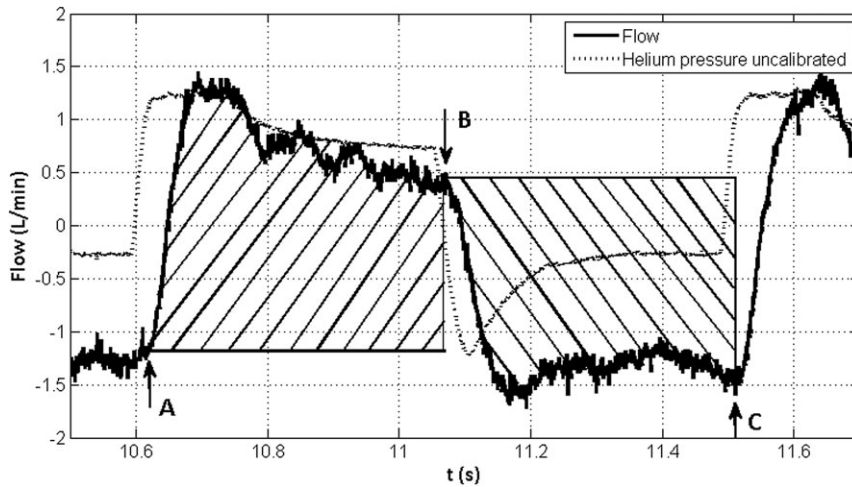
FIG. 2. Flow waveform (solid line) and balloon catheter helium pressure (dotted line) are plotted against time. The area integrated under the solid line between points A and B indicates the volume displaced away from the tip of the balloon (upstream) during inflation. The area integrated above the solid line between points B and C indicates the volume suctioned from the tip of the balloon during deflation. The flow scale indicates negative value at the onset of inflation due to the deflation of the previous cycle.

using ProAnalyst (Xcitex Inc., Cambridge, MA, USA). The diameter is defined as the projected width of the balloon on the measuring plane, derived as the distance between the balloon walls at each of the above-mentioned locations, and was followed throughout one cycle. Also, the duration of inflation and deflation were calculated from the images composing the videos of the operating balloon. The beginning and end of inflation and deflation were established by observing the videos at slow speed and determining the instances at which the IAB wall first moves following the onset of inflation and deflation, respectively.

Calibrations

The flow probes were calibrated using the timed collection technique at 15 different flow rates and the pressure transducers were calibrated using the column of fluid method at four different pressures. Both flow and pressure were calibrated in a range of values which is physiological in a human the AO. Diameter calibration, in ProAnalyst, was made through assigning 2.8 cm to the external diameter of the AO. In order to estimate and take into consideration the effect of light refraction through the silicone rubber tube filled up with water, four rigid objects of 1.91, 1.65, 0.81, and 0.52 cm in diameter were inserted in the tube and recorded using the high-speed camera. The size of each object was then measured in ProAnalyst to establish the overestimation due to the light refraction. The diameters were found to be 2.068, 1.782, 0.841, and 0.525 cm, respectively. These measurements resulted in refraction coefficients of 1.08, 1.08, 1.04, and 1.01, respectively, and in this work we used a refraction coefficient of 1.08 corresponding to the balloon maximum inflation diameter of ~1.7 cm.

Statistics and reproducibility

Results are reported as mean values ± standard deviation. *P* values < 0.05 with two-tailed Student's *t*-test were considered statistically significant.

To establish the experimental variability, the diameter waveforms at the base, center, and tip from five recordings of the IAB during counterpulsation at each position, horizontal and 45°, were examined. The coefficient of variation (C_v) was calculated as the standard deviation divided by the average value throughout the cycle. Maximum C_v of the five recordings, at the three sites and the two positions, was found to be 0.27 (center of IAB, at 45°). As $C_v < 1$, the recorded data were deemed low variance.

RESULTS

Duration of inflation and deflation

Changing the operating position from 0 to 45°, the duration of inflation decreased by 15.5% (0.275 ± 0.002 vs. 0.232 ± 0.009 s, $P < 0.01$), and the duration of deflation increased by 35% (0.309 ± 0.015 vs. 0.417 ± 0.008 s, $P < 0.01$).

Diameter

Base of the balloon

The diameter waveforms corresponding to the base of the balloon at 0 and 45° are shown in Fig. 3C.

Following inflation peak diameter at 45°, the base of the balloon reached a local minimum 0.044 s earlier than at the horizontal position. The onset of deflation is 0.007 s earlier at 45° than that at the horizontal position.
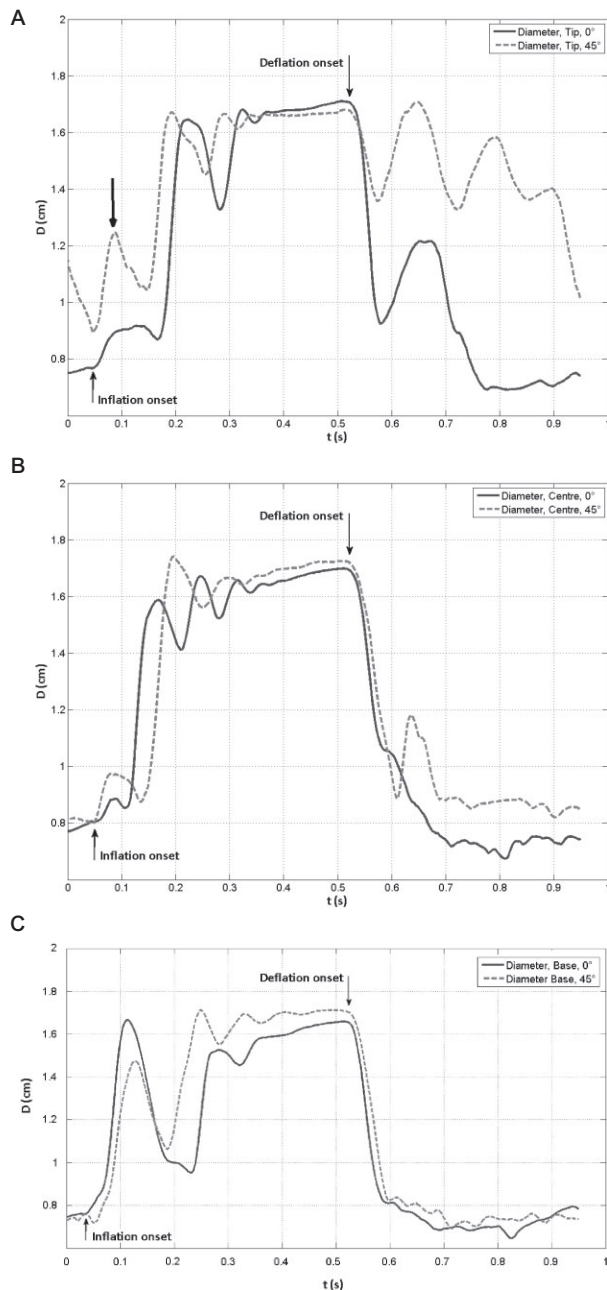
FIG. 3. Diameter at the horizontal (solid line) and at 45° (dashed line) at the tip (A), center (B), and base (C) of the balloon. The diameter waveforms of the base and center of the IAB are similar in shape at 0 and 45°, while the tip shows different dynamics of both inflation and deflation. Diameter at 45° is always larger during deflation at all parts of the balloon. Thick arrow in (A) indicates an earlier and larger peak tip diameter at 45 than 0°.

Center of the balloon

The diameter waveform at the center of the balloon shown in Fig. 3B follows a similar pattern at the 0 and 45° positions.

The deflation patterns between the two positions present one main difference: at 0.64 s, the diameter waveform shows a peak at 45°, which is absent at the horizontal position. The difference in diameter related to this peak is 0.29 cm (1.18 ± 0.22 vs. 0.89 ± 0.04 cm, $P < 0.05$) as shown in Fig. 3B.

Tip of the balloon

The diameter at the tip of the balloon shows clear differences between the horizontal and angled position (Fig. 3A).

The main differences between the two waveforms are found at the beginning of inflation and throughout the deflation process. After the onset of inflation, the diameter associated to the tip of the IAB presents an initial peak before increasing steeply: the maximum value of this peak is 0.92 ± 0.13 cm at 0° and 1.25 ± 0.17 cm at 45°. Also, the inflation peak is reached 0.029 s earlier at 45° than at 0°.

At the tip of the IAB, the onset of deflation is not altered and the diameter begins to decrease at the same time of the respective cycle at 0 and 45°. However, the diameter exhibits an increase when it reaches 0.93 ± 0.03 and 1.36 ± 0.05 cm at 0 and 45°, respectively. This increase brings the diameter value to 1.22 ± 0.05 and 1.71 ± 0.02 cm at 0 and at 45°, respectively. Then the diameter reached its minimum value of 0.69 ± 0.05 cm at a horizontal position, while at 45°, following a plateau, a further increase was observed before the diameter reached its minimum value of 1.02 ± 0.12 cm. It was observed that at 45°, the tip of the balloon remained partially inflated and did not decrease below 1.37 ± 0.04 cm (60% of AO internal diameter) until 0.91 s, which is only 0.04 s before the following inflation cycle.

Pressure pulse

PPi did not change markedly along the balloon (Table 1), but decreased throughout the IAB by around 9% from 0 to 45° (235 ± 1 vs. 214 ± 4 mm Hg, $P < 0.01$). The base and center of the IAB generated higher PPi at the horizontal position, 235 mm Hg, than the tip (2.13%, $P < 0.05$) did. At 45°, PPi was 215 mm Hg, 3.26% higher than that at the tip ($P = 0.07$). Similarly, PPd along the balloon remained almost unchanged, but decreased homogeneously with the angle (Table 1). At the center, PPd decreased by 14.7% (150 ± 3 vs. 128 ± 1 mm Hg, $P < 0.01$) from 0 to 45°. The pressure difference between the tip and base during one cycle is shown in Fig. 4. The main dissimilarity of the pressure

TABLE 1. *Pulse pressure due to inflation (PPi) and due to deflation (PPd) measured at the tip, center, and base of the balloon, for the horizontal and 45° positions*

		Horizontal	45°	% Change
PPi	Tip	230 ± 1 mm Hg	208 ± 4 mm Hg	−9.6
	Center	235 ± 1 mm Hg	214 ± 4 mm Hg	−9
	Base	235 ± 1 mm Hg	215 ± 5 mm Hg	−8.5
PPd	Tip	147 ± 3 mm Hg	130 ± 3 mm Hg	−11.6
	Center	150 ± 3 mm Hg	128 ± 1 mm Hg	−14.7
	Base	146 ± 1 mm Hg	122 ± 1 mm Hg	−16.4
VUTVi		0.41 ± 0.03	0.40 ± 0.04	−2.5
VUTVd		0.33 ± 0.03	0.28 ± 0.04	−15.2

VUTVi and VUTVd indicate volume displaced to and sucked from upstream the balloon, divided by the nominal balloon volume, during inflation and deflation, respectively.

difference between the horizontal (Fig. 4A) and angulated (Fig. 4B) position was the presence of a peak following the onset of deflation at 45°, which was not found at 0°.

Flow

VUTVi and VUTVd are reported in Table 1. Changing balloon position from 0° to 45° VUTVi decreased by 2.5% (0.41 ± 0.03 vs. 0.40 ± 0.04,
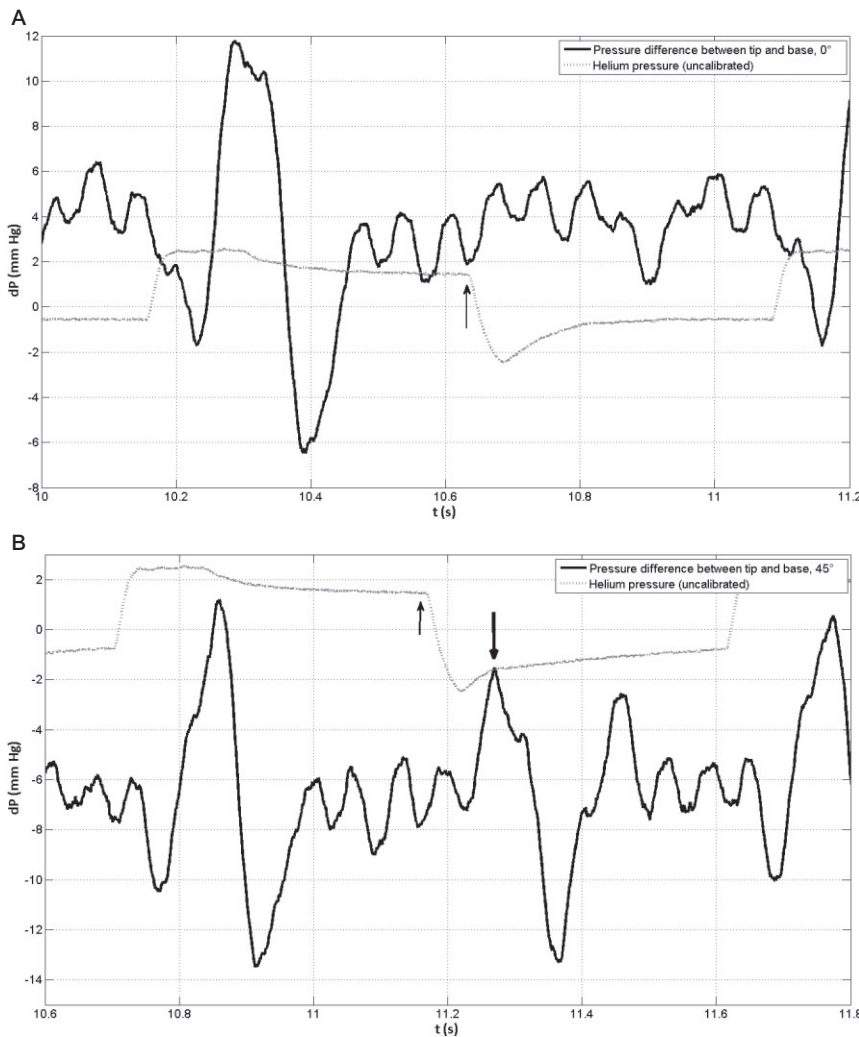
FIG. 4. Pressure difference between tip and base of the balloon (solid line) at a horizontal position (A) and at 45° (B), with the IABP uncalibrated helium pressure (dotted line). A clear peak is visible and indicated by the downwards pointing arrow immediately after deflation onset at 45° but missing at 0°. This peak indicates that at 45°, immediately after deflation onset as indicated by the upward pointing arrows, the pressure decreases more steeply at the base than at the tip.

$P = 0.6$) and VUTVd decreased by 15.2% (0.33 ± 0.03 vs. 0.28 ± 0.04, $P = 0.11$).

DISCUSSION

IAB diameter was measured for the first time at the base, center, and tip during counterpulsation. The results showed changes in the sequence of the balloon segments that fill and empty during inflation and deflation with varying balloon position from 0 to 45°. These changes were accompanied by changes in flow volume displacement and fluid pressure along the balloon. In particular, the deflation phase of the balloon was markedly influenced by a change in the operating angle as shown in Fig. 3A–C. The change in position induced a longer time for the IAB tip to deflate and a smaller deflation pressure pulse (Table 1), and consequently, decreased VUTVd (Table 1), all leading to reduced deflation effectiveness with increasing angle. Also during inflation, the diameter and pressure contours varied when operating the balloon at 45°. The inflation of the balloon tip in fact showed a larger early peak diameter, indicated by a thick arrow in Fig. 3A, which could have created an obstruction to the flow toward upstream circulation. Furthermore, the inflation diameter waveforms show that the IAB in a compliant tube performs differently compared with a stiff tube (5), highlighting the influence of the aortic elasticity on IAB dynamics.

Comparison with earlier studies

The present study was conducted in a compliant tube, and the results showed that when the balloon is placed horizontally, its diameter increases first at the base, then at the center, and finally at the tip (Fig. 5A). This finding contrasts with observations in earlier work by Bleifeld et al. (5) who observed that at a horizontal position, the IAB inflated first at its tip and base, almost simultaneously, and finally at its
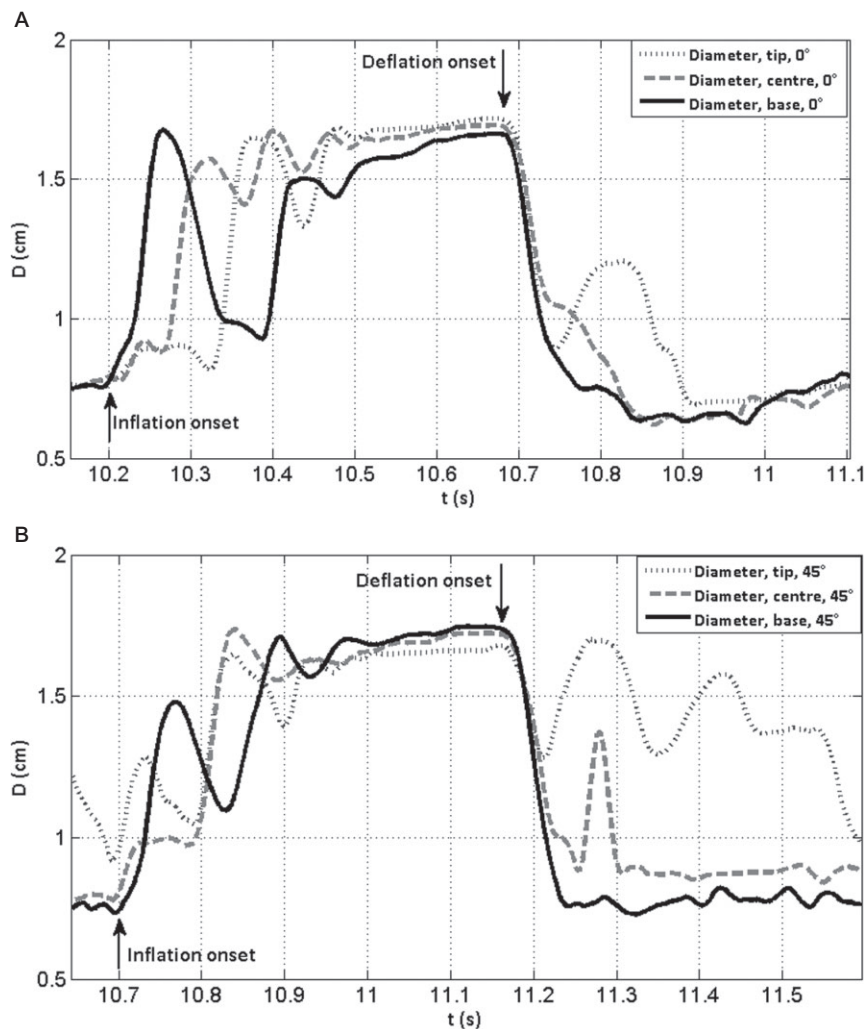

FIG. 5. Diameter, D, at the horizontal (A) and angled (B) positions for tip (dotted line), center (dashed line), and base (solid line) of the balloon. While at a horizontal position (A), the inflation peak appears first at the base followed by center and tip; at an angle (B), inflation is less linear and shows a first smaller inflation peak at the tip of the IAB.

center. The authors used a stiff tube accommodating the balloon, and concluded that free radial volume displacement of the fluid surrounding the balloon is prevented by the stiff tube, asserting that the initial inflation of the balloon happens at both ends. However, in this study, a silicone rubber tube, with size and compliance similar to those of the human AO, has been used for containing the IAB, and the diameter measurements showed that inflation starts at the base, follows at the center, and finally at the tip. We believe that the compliance of the flexible tube could accommodate part of the fluid displaced by the balloon, resulting in the IAB wall to start inflating at the base and continue toward the center and tip.

The duration of deflation was found to increase when changing the position from horizontal to 45°, in agreement with earlier work by Biglino et al. (7) at a pressure of 80 mm Hg. Biglino et al. reported an increase in duration of deflation by 17% (0.40 vs. 0.47 s, $P < 0.05$) when the balloon operated at an angle of 75° and an increase of 35% (0.309 vs. 0.417 s, $P < 0.05$) was found in the present study at 45°. However, Khir et al. (6) reported an overall-unchanged duration of deflation of 0.28 s between 0 and 60°.

The duration of inflation in this study is in agreement with earlier work by Khir et al. (6). The authors found 20% reduction in duration of inflation from 0 to 60°, comparable with a reduction of 15% ($P < 0.05$) from 0 to 45° presented in this study, even though the duration of inflation at the horizontal position was slightly different (0.20 vs. 0.275 s). However, these results do not agree with those reported by Biglino et al. (7), who found that the duration of inflation does not vary significantly from 0 to 75°, on average 0.27 s. A possible explanation for the differences between the results of the aforementioned works is due to the experimental test bed

used in each experiment, because the performance of the IABP is known to be affected by the compliance of the aortic wall, as previously reported (13,14).

Inflation effectiveness

The results showed that when the balloon is operated at 0°, its diameter increases first at the base, then at the center, and finally at the tip, which has a smaller diameter compared with the center and base for the first part of inflation, until 0.185 s into inflation (Fig. 5A). When operating the IAB at 45°, the tip diameter of the balloon (Fig. 5B) is larger than the rest of the balloon until 0.05 s into inflation. Hence, the obstruction to the flow displaced upstream, imposed by the tip of the IAB during this phase, could have more detrimental effects at an angle compared with the horizontal position. This is expected to negatively affect VUTVi, although in this work it decreased only by 2.5% ($P = 0.6$) at 45°.

Deflation effectiveness

This study offers an important focus on the deflation phase, which has been less studied in the past years and deserves a more thorough understanding. In fact, according to Cheung et al. (15), this might actually be the main advantage of the IAB, acting for reducing ventricular afterload.

It was confirmed that an increase in the operating angle of the balloon induces a decrease in both VUTVd (Table 1) and deflation pressure pulse (Table 1), thus compromising fundamental hemodynamic benefits associated with balloon deflation. Comparing the diameter waveforms at the tip of the balloon, at 0° and at 45°, does shed some light on this process (Fig. 6). Following the onset of deflation, the negative slope of the diameter waveform at the tip of the balloon is smaller at 45° than at 0°, with the diameter decreasing in 0.055 s by 0.33 cm at 45° and
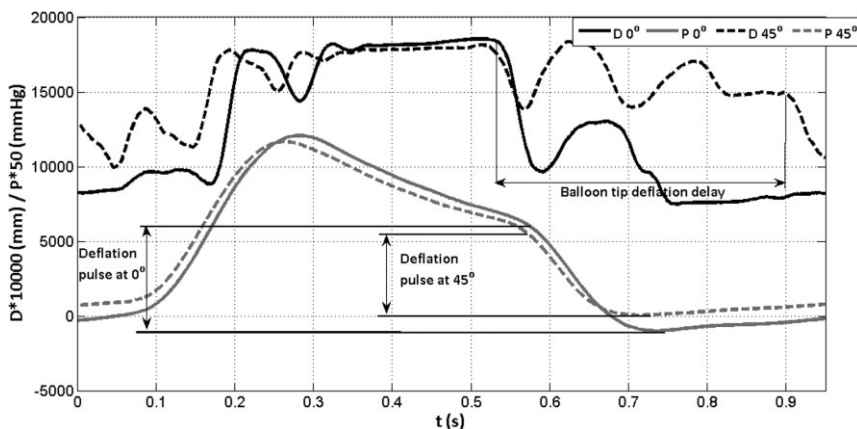

FIG. 6. Diameter (D, black line) and pressure (P, gray line) waveforms at the tip of the balloon at 0° (solid line) and 45° (dotted line). Dashed and solid vertical arrows indicate the reduced deflation pulse at the angled and horizontal positions, respectively, while the horizontal arrow indicates the potential cause related to this loss, a delayed deflation of IAB tip.

0.77 cm at 0°. In addition, the tip of the balloon reached the minimum deflation diameter at approximately 0.19 s later at 45° compared with the time at 0°. Both effects led to a smaller deflation pressure pulse.

The quantification of this delay in IAB deflation in vitro could be useful when projected in clinical settings and particularly in patients with higher heart rates for whom systole might start before the IAB is fully deflated and the base diameter has not yet reached its minimum. An earlier onset of deflation might counterbalance this loss in reduced afterload, although this may compromise the benefit of inflation, which would be shortened in this case.

Because diameter waveforms showed that the base is the first IAB segment to completely deflate at an angle, while the tip is only partially emptied, the helium flow can be expected to encounter a higher resistance flowing back toward the pump and therefore the balloon will empty, especially at the tip, at a slower pace. This could provide an explanation to the loss in efficiency that is reflected in a reduction in VUTVd. An additional reason for the deterioration in VUTVd and deflation pulse at an angle might be due to the increased resistance imposed on flow suction from upstream with increasing angle. As already mentioned, when the IAB is tilted it starts deflating from the base while the tip is the last segment to deflate (Fig. 5B), which suggests that the tip segment of the IAB remains with the largest diameter throughout the deflation phase and thereby imposes a larger obstruction to flow suctioned from upstream (9) than it does at 0°.

The pressure difference between the tip and base of IABP appears to play a role in the performance of inflation and deflation. When the balloon is at 0°, no sharp change in the pressure difference is observed after the onset of deflation, confirming the observations of the diameter measurements and suggesting that the deflation starts simultaneously at the tip and base of the balloon (Fig. 4A). Differently, when the balloon is at 45°, an increase in the pressure difference between the tip and base is observed immediately after deflation onset (Fig. 4B), suggesting that the hydrostatic pressure difference forces deflation to start at the base and proceed toward the tip.

Experimental and measurement considerations

The values of pulse pressure presented in Table 1 are exceptionally higher than those observed in vivo. This could be due to a number of reasons: (i) the experimental setup is simple, with resistances and compliances simulated as lumped parameters; (ii) the distance traveled by the waves generated by IAB inflation and deflation is rather short, compared with

that in vivo, which enhances the magnitude of reflected waves causing an increase in pressure; (iii) the volume of fluid used in this study is less than the volume of blood in the human body, and therefore the effect of balloon inflation and deflation will be magnified in this smaller volume. Nevertheless, replicating in vivo pressure or flow waveforms was not the focus of the current work, but rather analyzing IAB wall movements at the horizontal and angled positions.

In this work, the diameter of the IAB was taken as the projected width of the balloon on the measuring plane, derived as the distance between the balloon walls. The camera was always placed at a right angle to the IAB long axis, but the possibility that the IAB membrane collapses on a plane that forms an angle to the measuring plane cannot be excluded. Therefore, the projected diameter of an empty balloon on the measuring plane may not show the images as the thickness of the two walls only. Further, when the balloon is empty, it does not collapse flat, but furled along the IAB catheter, resulting in a radius of approximately 0.85 cm. The small hydrostatic pressure difference between the top and the bottom walls of the tube is not expected to affect the shape of the IAB cross-sectional area.

The refraction factor determined in this study takes into account the distortion effects of both the silicone tube and water together, and hence corrects for their combined effect. We note that the refraction factor was determined by placing the rigid object inside the silicone tube only at a single distance away from the wall of the silicone tube, while the balloon walls will be moving at a varying distance from the silicone tube walls during inflation and deflation. Given that the distance traveled by the walls of the IAB is small (≅0.85 cm, radius of the IAB cross-sectional area), we expect that the different refractions would probably be inconsequential to our results.

The refraction coefficients for the different-sized objects indicated that different stages of the balloon inflation and deflation may have needed different refraction coefficients. However, the difference between the minimum and maximum refraction, corresponding to the minimum and maximum balloon diameter at full inflation and deflation, is <7%. This value drops to 3.5% during balloon inflation and deflation. Given that the present work is not concerned with the exact value of diameters, but rather with a comparison between the behavior of the diameter when the balloon is operated at the horizontal and at an angle, we deemed that using a refraction factor of 1.08 representing the largest balloon

diameter is appropriate. The above small errors have been systematically applied to the balloon diameter both at the horizontal and at an angle, and should not affect our observations or conclusions.

Limitations

In this study, the IAB has been filmed and analyzed just on the frontal plane and consequently only information about the projected diameter on that plane was obtained. Additional simultaneous recording of the balloon wall movement from the top and side planes could have provided further information about the shape of the cross-sectional area to make the analysis more complete. However, we do not anticipate that this added experimental complexity would significantly change the general conclusions derived from the present study.

The current experimental setup did not include a physical model of the coronary circulation. This would have been useful to study the effect of angulation on coronary flow. However, given that the focus of this study is placed on studying the IAB wall patterns of inflation and deflation at 0 and 45°, an inclusion of a coronary circulation model would not have likely changed the results or the conclusions drawn from the current work. A further improvement to the current experimental setup could be the adjustment of the compliance distribution upstream and downstream the IAB, in order to yield physiological *total* compliance and not only physiological *distribution*, as done at present.

CONCLUSION

Intra-aortic balloon diameter measurements provided rationale to our earlier observations of reduced intra-aortic balloon pump efficacy when operated at an angle to the horizontal. Measurements of pressure along the balloon and flow provided further evidence for such reduced IABP performance.

At 45°, the deflation is slower and the deflation pressure pulse, indicating the reduction in end-diastolic pressure in the clinical setting, is smaller than that found at 0°. Although this is outside the scope of this work, slower deflation may well require adjustments to the IABP optimal triggering time in the clinical setting.

Also, at 45° the IAB tip inflates before the rest of the balloon, providing further resistance against the flow displaced during inflation. This resulted in the decreased VUTVi at 45°, resembling reduced flow toward the coronary circulation in vivo.

The results of this work, although in vitro, have clinical implications and suggest that from the efficacy viewpoint, IABP patients are best nursed in the horizontal position. As most patients using the IABP need to be nursed in the semi-recumbent position, it seems that modifications to the balloon shape, filling patterns, and inflation/deflation timing at the various angles, require further investigation to achieve the maximum benefit of this therapy.

REFERENCES

1. Thomas PJ, Paratz JD, Stanton WR, Deans R, Lipman J. Positioning practices for ventilated intensive care patients: current practice, indications and contraindications. *Aust Crit Care* 2006;19:122–32.
2. Li TST, Joynt GM, So HY, Gomersall CD, Yap FHY. Semi-recumbent position in ICU. *Crit Care & Shock* 2008;11:61–6.
3. Kollef MH. Prevention of hospital-associated pneumonia and ventilator-associated pneumonia. *Crit Care Med* 2004;32:1396–405.
4. Lorente L, Blot S, Rello J. Evidence on measures for the prevention of ventilator-associated pneumonia. *Eur Respir J* 2007;30:1193–207.
5. Bleifeld W, Meyer-Hartwig K, Irnich W, Bussmann WD, Meyer J. Dynamics of balloons in intraaortic counterpulsation. *Am J Roentgenol Radium Ther Nucl Med* 1972;116:155–64.
6. Khir AW, Price S, Hale C, Young DA, Parker KH, Pepper JR. Intra-aortic balloon pumping: does posture matter? *Artif Organs* 2005;29:36–40.
7. Biglino G, Kolyva C, Whitehorne M, Pepper JR, Khir AW. Variations in aortic pressure affect the mechanics of the intra-aortic balloon: an in vitro investigation. *Artif Organs* 2010;34:546–53.
8. Biglino G, Whitehorne M, Pepper JR, Khir AW. Pressure and flow-volume distribution associated with intra-aortic balloon inflation: an in vitro study. *Artif Organs* 2008;32:19–27.
9. Khir AW, Bruti G. Intra-aortic balloon shape change: effects on volume displacement during inflation and deflation. *Artif Organs* 2013;37:E88–95.
10. Westerhof N, Bosman F, De Vries CJ, Noordergraaf A. Analog studies of the human systemic arterial tree. *J Biomech* 1969;2:121–43.
11. Khir AW. What is it with patient's posture during intra aortic balloon pump therapy? *Artif Organs* 2010;34:1077–81.
12. Kolyva C, Biglino G, Pepper JR, Khir AW. A mock circulatory system with physiological distribution of terminal resistance and compliance: application for testing the intra-aortic balloon pump. *Artif Organs* 2010;36:E62–70.
13. Papaioannou TG, Mathioulakis DS, Stamatelopoulos KS, et al. New aspects on the role of blood pressure and arterial stiffness in mechanical assistance by intra-aortic balloon pump: in-vitro data and their application in clinical practice. *Artif Organs* 2004;28:717–27.
14. Papaioannou TG, Mathioulakis DS, Nanas JN, Tsangaris SG, Stamatelopoulos SF, Moulopoulos SD. Arterial compliance is a main variable determining the effectiveness of intra-aortic balloon counterpulsation: quantitative data from an in vitro study. *Med Eng Phys* 2002;24:279–84.
15. Cheung AT, Savino JS, Weiss SJ. Beat-to-beat augmentation of left ventricular function by intraaortic counterpulsation. *Anesthesiology* 1996;84:545–54.